

Eg5 Causes Elongation of Meiotic Spindles When Flux-Associated Microtubule Depolymerization Is Blocked

Mimi Shirasu-Hiza,^{1,*} Zachary E. Perlman,²
Torsten Wittmann,³ Eric Karsenti,⁴
and Timothy J. Mitchison²

¹Department of Microbiology and Immunology
Stanford University
Stanford, California 94305

²Department of Systems Biology
Harvard Medical School
200 Longwood Ave
Boston, Massachusetts, 02115

³Department of Cell Biology
Scripps Research Institute
La Jolla, California 92037

⁴Cell Biology and Cell Biophysics Programme
European Molecular Biology Laboratory
Heidelberg
Germany

Summary

In higher eukaryotes, microtubules (MT) in both halves of the mitotic spindle translocate continuously away from the midzone in a phenomenon called poleward microtubule flux. Because the spindle maintains constant length and microtubule density, this microtubule translocation must somehow be coupled to net MT depolymerization at spindle poles. The molecular mechanisms underlying both flux-associated translocation and flux-associated depolymerization are not well understood, but it can be predicted that blocking pole-based destabilization will increase spindle length, an idea that has not been tested in meiotic spindles. Here, we show that simultaneous addition of two pole-disrupting reagents p50/dynamitin and a truncated version of Xklp2 results in continuous spindle elongation in *Xenopus* egg extracts, and we quantitatively correlate this elongation rate with the poleward translocation of stabilized microtubules. We further use this system to demonstrate that this poleward translocation requires the activity of the kinesin-related protein Eg5. These results suggest that Eg5 is responsible for flux-associated MT translocation and that dynein and Xklp2 regulate flux-associated microtubule depolymerization at spindle poles.

Results and Discussion

Simultaneous Addition of p50 and Xklp2 Tail Results in Meiotic Spindle Elongation

Flux-associated MT translocation might be caused by equilibrium microtubule polymer dynamics, as originally proposed in the treadmilling model [1], or it might be caused by a plus end-directed motor protein [2, 3]. One way to distinguish these hypotheses would be to block depolymerization at poles and ask if translocation stops

or if the spindle elongates. In an elegant experiment in *Drosophila* embryos, microinjection of antibodies against a kin I kinesin resulted in qualitatively longer spindles at the site of injection [4]. To date, this experiment has not been possible in *Xenopus* extract spindles as a result of a lack of reagents blocking depolymerization at poles. *Xenopus* extracts recapitulate egg meiosis II spindle assembly [2, 5] and provide a useful, biochemically manipulatable system for quantitative study of poleward microtubule flux. In contrast to the *Drosophila* embryo, perturbation of the two known *Xenopus* kin I kinesins (XKCM1 and Xkif2) does not cause spindle elongation. Instead, spindles exhibit excessive microtubule polymerization around a spindle of unchanged pole-to-pole distance (T.J. Mitchison et al., submitted; and [6]).

Here, we apply two pole-disrupting reagents, p50/dynamitin and GST-Xklp2 tail, to produce dramatically elongated spindles (original observation by R. Heald and C. Walczak, personal communication) and quantitatively correlate the rate of this elongation with the rate of microtubule translocation. p50/dynamitin (p50) is a 50 kDa dynactin component that in excess disrupts the dynein-dynactin complex in vitro and causes unfocused spindle poles in both cells and *Xenopus* egg extract [7, 8]. Xklp2 is a plus end-directed kin N kinesin thought to be involved in spindle pole separation and spindle assembly [9]; addition of a truncated version (Xklp2 tail) also disrupts spindle poles in *Xenopus* extracts [7, 8]. A likely target for both treatments is TPX2, a protein involved in pole assembly that requires both dynein and Xklp2 for localization [10].

Figure 1A shows polarized-light microscopy images for spindles treated with buffer, p50, Xklp2 tail, or p50 and Xklp2 tail together (p50+Xklp2 tail). Treatment with p50 alone [8, 11] or p50+Xklp2 tail resulted in spindles with defocused poles. However, spindles that were treated with p50+Xklp2 tail also elongated continuously for at least 15–30 min (see Movie 1 in the Supplemental Data available with this article online). Several frames from two sample movies, one treated with buffer and the other with p50+Xklp2 tail, are shown (Figure 1B).

p50+Xklp2 Tail Spindle Elongation Occurs at the Rate of Poleward MT Translocation

We hypothesized that this spindle elongation is due to flux-associated poleward translocation of microtubules past the original spindle periphery, implying that flux-associated MT depolymerization must be blocked. If so, the rate of spindle elongation should closely correlate with the rate of microtubule translocation for individual spindles. To test this, we measured both rates simultaneously in individual spindles by using fluorescent-speckle microscopy (FSM) [12]. Sample kymographs are shown for a buffer-treated control spindle and a spindle treated with p50+Xklp2 tail (Figure 2A). The average rate of microtubule translocation was similar for all four types of experimental treatment (control: 2.5 ± 0.2 $\mu\text{m}/\text{min}$, $n = 5$; p50: 2.9 ± 0.4 , $n = 5$; Xklp2 tail: $2.5 \pm$

*Correspondence: mshirasu@stanford.edu

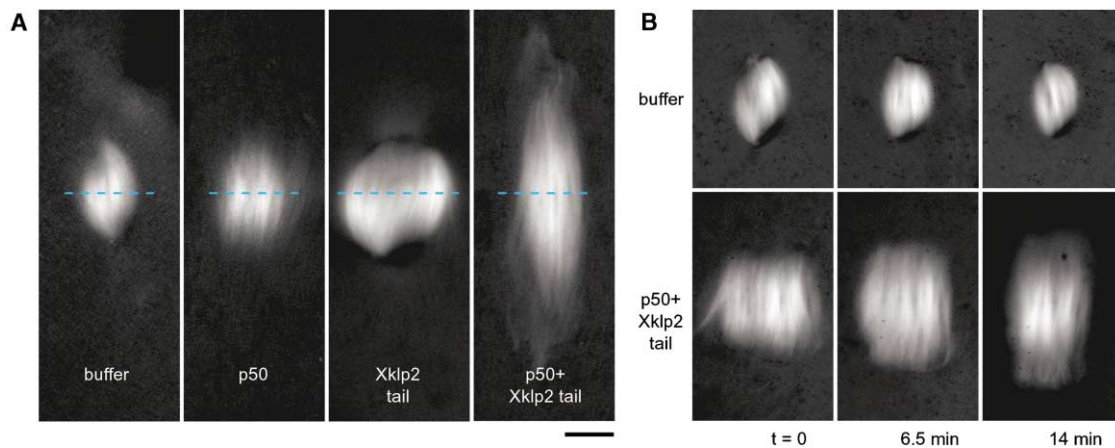


Figure 1. Addition of Both p50 and Xklp2 Tail Causes Spindle Elongation

Meiotic spindles were assembled by addition of demembrated sperm nuclei to *Xenopus* egg extract and visualized with polarized-light microscopy.

(A) Examples of spindle morphology treated with buffer, p50, Xklp2 tail, and p50+Xklp2 tail together are shown here. Blue dashed line indicates location of the spindle midzone.

(B) Frames from two time-lapse movies show that, unlike the control spindle, the spindle treated with p50+Xklp2 tail undergoes continuous elongation. The scale bar represents 30 μm .

0.26 $\mu\text{m}/\text{min}$, $n = 4$; p50+Xklp2 tail: $1.8 \pm 0.7 \mu\text{m}/\text{min}$, $n = 10$; Figure 2B). Only spindles treated with both p50 and Xklp2 tail underwent significant elongation, at an average rate of $1.4 \pm 0.5 \mu\text{m}/\text{min}$. In these spindles, the rates of spindle elongation and microtubule translocation were strongly correlated (Figure 2C).

p50+Xklp2 tail treatment also induced elongation in extract spindles assembled around DNA-coated beads, independent of exogenous centrosomes [13] (Figure S1). This elongation rate correlated with the rate of MT translocation measured by photoactivation experiments. In addition, the photoactivation mark did not move relative to the pole during elongation, supporting the hypothesis that elongation results from blocked MT depolymerization rather than growth of minus ends.

p50+Xklp2 tail treatment appears to specifically block pole-associated MT depolymerization while allowing continued poleward MT translocation. In FSM movies, spindle microtubules (fluorescent speckles) stably translocate from the spindle midzone past the original spindle periphery (see Movie 2). Similarly, kymographs of p50+Xklp2-treated spindles show a persistence of MT minus ends at the spindle periphery (Figure 2A). Cytoplasmic microtubule density is not dramatically increased, suggesting that this treatment does not directly affect microtubule dynamics. Because added Xklp2 tail protein localizes to the spindle periphery (data not shown), it is possible that Xklp2 tail binds residual pole complexes after p50 treatment and inhibits or delocalizes their MT depolymerizing activity there. Given this, it will be interesting to use this system to test pole localization of different MT depolymerizing factors like kin I family members and to probe their role in flux-associated depolymerization. Recent evidence from a similar system points to a possible role for the kin I kinesin Xkif2 [6].

Spindle Elongation Is Caused by Poleward Microtubule Translocation Driven by Eg5

We used these elongating spindles to probe the mechanism of MT translocation underlying poleward flux. Uncoupling of depolymerization and MT translocation, as seen here, indicates that translocation is not likely to be driven by a depolymerization-based mechanism. Instead, a motor protein might effect poleward MT sliding [2, 3]. The plus end-directed tetramer kinesin Eg5 is an excellent candidate for flux-associated translocation activity but has been technically difficult to test directly because complete depletion or inhibition of Eg5 results in monoastrial MT structures that do not undergo poleward flux. However, recent experiments have shown that inhibition of dynein and Eg5 together rescues the bipolar phenotype [14, 15].

Here, we use two inhibitors, the slowly hydrolyzable ATP analog AMPPNP and the specific Eg5 inhibitor monastrol [17], to demonstrate that Eg5 is responsible for spindle elongation and poleward MT translocation. AMPPNP is known to inhibit kinesin- and dynein-dependent transport along microtubules. Though a nonspecific inhibitor, AMPPNP was until recently the only known inhibitor of poleward MT translocation in *Xenopus* egg extract spindles [2, 16]. In the presence of 1 mM AMPPNP, both microtubule translocation and spindle elongation induced by p50+Xklp2 tail treatment were completely inhibited (Figure 3A). The average rate of poleward translocation was $0.02 \pm 0.02 \mu\text{m}/\text{min}$ and the average rate of spindle elongation was $0.02 \pm 0.03 \mu\text{m}/\text{min}$ ($n = 5$).

Because Eg5 has recently been demonstrated to be required for flux-associated poleward microtubule translocation in *Xenopus* egg extract spindles [15], we tested the effects of monastrol on p50+Xklp2 tail-induced spindle elongation. We found that monastrol treatment here inhibited both poleward MT translocation and spin-

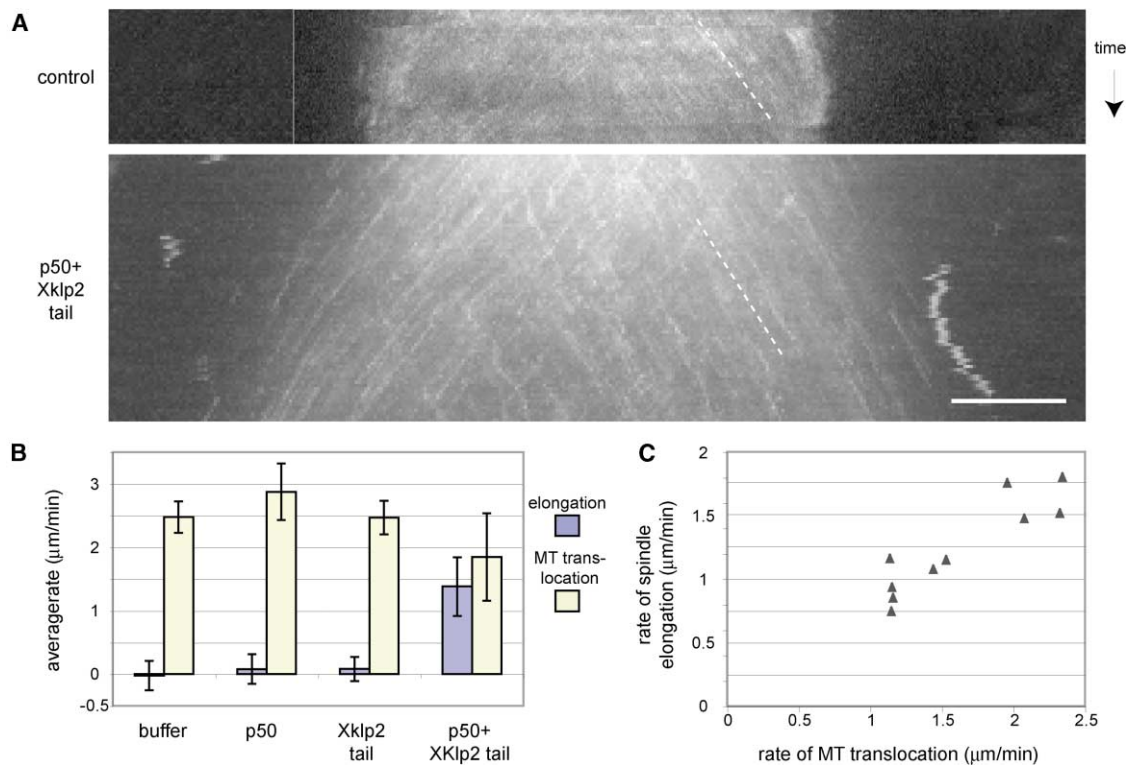


Figure 2. The Rate of Spindle Elongation in p50/Xklp2 Tail Spindles Correlates with the Rate of Poleward Microtubule Translocation
Microtubule translocation rate was monitored in spindles treated with buffer, p50, Xklp2 tail, or p50+Xklp2 tail by using fluorescent speckle microscopy (FSM).
(A) Sample kymographs are shown here for one spindle treated with buffer (top) and one spindle treated with p50+Xklp2 tail (bottom). The scale bar represents 10 μm.
(B) This graph of average rates of microtubule translocation and spindle elongation shows that each type of spindle had normal rates of poleward microtubule translocation, but only p50+Xklp2 tail structures elongated significantly.
(C) Plot of translocation rate versus elongation rate for individual p50+Xklp2 tail spindles reveals a strong correlation.

dle elongation in p50+Xklp2 tail spindles. This effect was titratable over a range of monastrol concentrations with an IC50 of approximately 20 μM.

Taken together, these results suggest that p50+Xklp2 tail treatment selectively inhibits flux-associated microtubule depolymerization while allowing flux-associated MT translocation, resulting in continuously elongating spindles. We used this system to confirm that the kinesin Eg5 is responsible for poleward MT translocation and furthermore can perform work in the absence of depolymerization. This system might also be used to probe the mechanism of flux-associated depolymerization in meiotic *Xenopus* spindles. Possible mechanisms include direct depolymerization at minus ends—for example, powered by: a kin I kinesin, as supported by recent experiments in *Drosophila* embryos [4] and *Xenopus* egg extract [7]; MT severing by katanin, which is known to have a special role in meiotic spindles [18]; or a meiotic pole environment that facilitates plus end destabilization to cause complete loss of (nonkinetochore) MTs. Because the elongating spindles we describe here are robust and technically straightforward to effect and do not induce general cytoplasmic MT polymerization, this should represent a useful and biochemically tractable system in

which to test the role of these mechanisms in flux-associated depolymerization.

Experimental Procedures

Spindle Assembly in *Xenopus* Egg Extract

All experiments were performed with fresh cytostatic factor (CSF)-arrested *Xenopus* egg extracts prepared according to [19]. Cycled sperm-nucleated spindle assembly reactions were performed as previously described [13, 20].

Reagents Added to Spindle Assembly Reactions

Tubulin was labeled with tetramethyl- or X-rhodamine (Molecular Probes) as previously described [21]. Rhodamine-labeled tubulin was added at 0.5 μM for visual analysis of microtubule structures and 10–50 nM for speckle microscopy.

Purified recombinant p50/dynamitin, a generous gift from E. Salmon (UNC Chapel Hill, NC), was added to a final concentration of ~1 mg/ml either at the beginning of the interphase incubation at room temperature or simultaneously with the addition of CSF-arrested extract. A plasmid construct of glutathione-S-transferase fusion protein containing the COOH-terminal domain of Xklp2 (GST-Xklp2 tail) was a generous gift from C. Walczak (Indiana University, IN). Purified recombinant GST-Xklp2 tail was added to extract at a final concentration of 0.125 mg/ml after at least 60 min of incubation with added CSF-arrested extract or postspindle assembly.

AMPPNP was purchased from Sigma and used at a final concen-

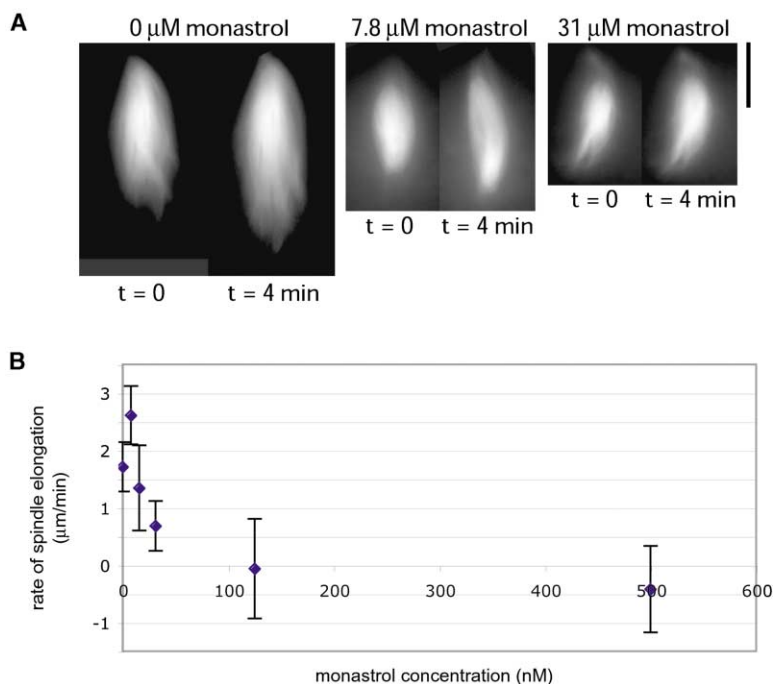


Figure 3. p50/Xklp2 Tail-Induced Spindle Elongation Requires Eg5-Driven Microtubule Translocation

Spindles were treated with p50+Xklp2 tail for inducing elongation and then treated with varying amounts of monastrol, a specific inhibitor of Eg5.

(A) Still images from fluorescence movies. The scale bar represents 20 μM .

(B) Inhibition of spindle elongation by monastrol is titratable between 3.125 and 500 μM . The IC₅₀ for spindle elongation appears to be ~ 20 μM .

tration of 1 mM. Monastrol was a gift from Z. Maliga and was diluted into DMSO before addition to extract. Final DMSO concentration was 0.5%. It was important to mix the extract well after monastrol addition. For all conditions, total dilution of the extract did not exceed 10% total volume.

Assays for Spindle Elongation and Poleward Microtubule Flux

Polarized light microscopy was performed on an inverted Nikon TE300 microscope with 20 \times objective and no binning. ~ 5 μl of extract was thinly spread with a pipette tip on a large (22 \times 22 mm) coverslip affixed to an aluminum holder and covered with ~ 250 μl of mineral oil, protecting the sample from evaporation but allowing free gas transfer, while the sample was observed from below with a 20 \times objective. Control spindles prepared in this way were observed to last at least 1 hr with no change in morphology. Images were acquired using a CCD detector (Orca ER camera, Hamamatsu Photonics) and Metamorph software (Universal Imaging, Westchester, PA). For time-lapse movies, we used exposures of 750 ms, with no binning, at 20 s intervals.

Fluorescent-speckle microscopy (FSM) experiments were performed on an upright Nikon E-600 or E-800 conventional wide-field fluorescence light microscope with 60 \times or 100 \times Plan apo objectives or on a TE300 Nikon inverted microscope outfitted with a Yokogawa spinning disk confocal unit with 60 \times or 100 \times Plan apo objectives. Samples were prepared in conventional squashes between an 18 \times 18 mm glass coverslip and glass slide sealed with melted VALAP (1:1:1 ratio of vaseline, lanolin, and paraffin). Typically, samples consisted of no less than 6–10 μl of extract to avoid spindle contact with glass surfaces. 1 $\mu\text{g}/\text{ml}$ Hoechst dye was added to help locate spindles by the UV fluorescence of their chromatin. All microscopes were equipped with cooled charge-coupled device cameras (wide-field: Princeton Instruments, Trenton, NJ; confocal: Hamamatsu Photonics) controlled by MetaMorph software (Universal Imaging, Westchester, PA). For time-lapse movies, we used exposures of 200–500 ms (bin = 2) with time intervals of 5–10 s.

All polarized light and FSM movies were analyzed by using the Kymograph function in Metamorph. Spindles were first aligned (to compensate for spindle movement in the field) with aligner, a custom-written automatic image registration program. For each kymograph, we drew a line of 5–10 pixels wide along the pole-to-pole spindle axis and created a kymograph by using the maximum fluo-

rescence in the region; we then drew lines following the movement of speckles or spindle edges on each kymograph. The angles of these lines were logged and analyzed in Microsoft Excel 2000 to extract rate information. The rate of flux can be highly variable even within the same spindle and the angle of the original kymograph line can make a large difference in final rates. Therefore, for flux analysis, we made 1–3 kymographs per sample and averaged the slopes of ~ 10 –40 lines per kymograph.

The effect of monastrol titration on spindle elongation was monitored by adding X-rhodamine-labeled tubulin and 1 $\mu\text{g}/\text{ml}$ Hoechst. Monastrol was diluted from a 100 mM stock into DMSO and added to a final concentration of 0.5% DMSO. Control reactions were performed with 0.5% DMSO. 10 μl of extract was squashed under an 18 \times 18 mm coverslip for each reaction; 200 ms exposures (60 \times , bin = 2) were taken every 20 s for 10–15 min. Spindle elongation was quantitated with Metamorph. After autothresholding, the Integrated Morphometry Analysis function was used on each stack for obtaining the length of the spindle at every time point. Results were logged in Microsoft Excel and plotted for each movie with the slope of the best-fit line giving the spindle elongation rate. For each concentration of monastrol, n = 3–7 spindles.

Supplemental Data

Supplemental Data including Supplemental Experimental Procedures, one additional figure, and two movies are available at <http://www.current-biology.com/cgi/content/full/14/21/1941/DC1/>.

Acknowledgments

We are grateful to Rebecca Heald and Claire Walczak for their original insight and for their gifts of reagents, as well as to Zoltan Maliga and Ted Salmon for their generosity with reagents. We also thank Lisa Cameron, Aaron Groen, Ted Salmon, and Christine Field for their help and camaraderie at Woods Hole; the Marine Biological Laboratory at Woods Hole, where many of these experiments were done; and Ann Yonetani and Becky Ward for advice on this manuscript. We are especially grateful to Justin Yarrow and Jennifer Timauer for their insightful comments. M.S.-H. was supported by a National Science Foundation Predoctoral Fellowship and Z.E.P. was supported by a Howard Hughes Medical Institute Predoctoral Fellowship. This work was funded in part by National Institutes of Health grant GM39565.

Received: July 13, 2004
Revised: September 13, 2004
Accepted: September 13, 2004
Published: November 9, 2004

References

1. Margolis, R.L., and Wilson, L. (1981). Microtubule treadmills—possible molecular machinery. *Nature* 293, 705–711.
2. Sawin, K.E., and Mitchison, T.J. (1991). Poleward microtubule flux mitotic spindles assembled in vitro. *J. Cell Biol.* 112, 941–954.
3. Sharp, D.J., Rogers, G.C., and Scholey, J.M. (2000). Roles of motor proteins in building microtubule-based structures: a basic principle of cellular design. *Biochim. Biophys. Acta* 1496, 128–141.
4. Rogers, G.C., Rogers, S.L., Schwimmer, T.A., Ems-McClung, S.C., Walczak, C.E., Vale, R.D., Scholey, J.M., and Sharp, D.J. (2004). Two mitotic kinesins cooperate to drive sister chromatid separation during anaphase. *Nature* 427, 364–370.
5. Cha, B.J., Error, B., and Gard, D.L. (1998). XMAP230 is required for the assembly and organization of acetylated microtubules and spindles in *Xenopus* oocytes and eggs. *J. Cell Sci.* 111, 2315–2327.
6. Gaetz, J., and Kapoor, T.M. (2004). Dynein/dynactin regulate metaphase spindle length by targeting depolymerizing activities to spindle poles. *J. Cell Biol.* 166, 465–471.
7. Echeverri, C.J., Paschal, B.M., Vaughan, K.T., and Vallee, R.B. (1996). Molecular characterization of the 50-kD subunit of dynactin reveals function for the complex in chromosome alignment and spindle organization during mitosis. *J. Cell Biol.* 132, 617–633.
8. Wittmann, T., and Hyman, T. (1999). Recombinant p50/dynactin as a tool to examine the role of dynactin in intracellular processes. *Methods Cell Biol.* 61, 137–143.
9. Boleti, H., Karsenti, E., and Vernos, I. (1996). Xklp2, a novel *Xenopus* centrosomal kinesin-like protein required for centrosome separation during mitosis. *Cell* 84, 49–59.
10. Wittmann, T., Wilm, M., Karsenti, E., and Vernos, I. (2000). TPX2, A novel *xenopus* MAP involved in spindle pole organization. *J. Cell Biol.* 149, 1405–1418.
11. Heald, R., Tournebise, R., Habermann, A., Karsenti, E., and Hyman, A. (1997). Spindle assembly in *Xenopus* egg extracts: respective roles of centrosomes and microtubule self-organization. *J. Cell Biol.* 138, 615–628.
12. Waterman-Storer, C.M., Desai, A., Bulinski, J.C., and Salmon, E.D. (1998). Fluorescent speckle microscopy, a method to visualize the dynamics of protein assemblies in living cells. *Curr. Biol.* 8, 1227–1230.
13. Heald, R., Tournebise, R., Blank, T., Sandaltzopoulos, R., Becker, P., Hyman, A., and Karsenti, E. (1996). Self-organization of microtubules into bipolar spindles around artificial chromosomes in *Xenopus* egg extracts. *Nature* 382, 420–425.
14. Gaglio, T., Saredi, A., Bingham, J.B., Hasbani, M.J., Gill, S.R., Schroer, T.A., and Compton, D.A. (1996). Opposing motor activities are required for the organization of the mammalian mitotic spindle pole. *J. Cell Biol.* 135, 399–414.
15. Miyamoto, D., Perlman, Z., Burbank, K., Groen, A., and Mitchison, T. The kinesin Eg5 drives poleward microtubule flux in *Xenopus* egg extract spindles. *J. Cell Biol.* in press.
16. Desai, A., Maddox, P.S., Mitchison, T.J., and Salmon, E.D. (1998). Anaphase A chromosome movement and poleward spindle microtubule flux occur at similar rates in *Xenopus* extract spindles. *J. Cell Biol.* 141, 703–713.
17. Mayer, T.U., Kapoor, T.M., Haggarty, S.J., King, R.W., Schreiber, S.L., and Mitchison, T.J. (1999). Small molecule inhibitor of mitotic spindle bipolarity identified in a phenotype-based screen. *Science* 286, 971–974.
18. Srayko, M., Buster, D.W., Bazirgan, O.A., McNally, F.J., and Mains, P.E. (2000). MEI-1/MEI-2 katanin-like microtubule severing activity is required for *Caenorhabditis elegans* meiosis. *Genes Dev.* 14, 1072–1084.
19. Murray, A.W. (1991). Cell cycle extracts. *Methods Cell Biol.* 36, 581–605.
20. Desai, A., Murray, A., Mitchison, T.J., and Walczak, C.E. (1999). The use of *Xenopus* egg extracts to study mitotic spindle assembly and function in vitro. *Methods Cell Biol.* 61, 385–412.
21. Hyman, A., Drechsel, D., Kellogg, D., Salser, S., Sawin, K., Steffen, P., Wordeman, L., and Mitchison, T. (1991). Preparation of modified tubulins. *Methods Enzymol.* 196, 478–485.